Journal of Hazardous Materials 164 (2009) 762–768

Contents lists available at ScienceDirect

Journal of Hazardous Materials

journal homepage: www.elsevier.com/locate/jhazmat

Study on photocatalytic performance and degradation kinetics of X-3B with lanthanide-modified titanium dioxide under solar and UV illumination

Jingjing Xu[a,b], Yanhui Ao[a,b], Degang Fu[a,b,*], Chunwei Yuan[a]

[a] State Key Laboratory of Bioelectronics, Southeast University, Nanjing 210096, China
[b] School of Chemistry and Chemical Engineering, Southeast University, Nanjing 210096, China

ARTICLE INFO

Article history:
Received 7 February 2008
Received in revised form 21 August 2008
Accepted 21 August 2008
Available online 7 September 2008

Keywords:
Photocatalysis
Kinetics
Titanium oxide
Scatchard plot
X-3B

ABSTRACT

The present work was focused on photocatalytic oxidation of the model molecule reactive brilliant X-3B by lanthanide-modified TiO_2 samples under artificial solar and UV irradiation. Experimental results showed that the TiO_2 samples doping with lanthanide (Ce and Gd) could greatly enhance the activity of pure TiO_2, and could extend the absorption range to visible region. The optimum doping amount was 0.2 and 0.5 at.% for Ce- and Gd-doped TiO_2 particles, respectively. The degradation kinetics of X-3B on Ce-doped TiO_2, Gd-doped TiO_2, and pure TiO_2 were studied as well. The results exhibited that the degradation of X-3B on all the samples were in accordance with the first-order model. The trend of apparent reaction rate constants k_{app} was as follows, Gd-doped TiO_2 > Ce-doped TiO_2 > pure TiO_2, under solar illumination. Scatchard plot analysis was used to evaluate the adsorption phenomena of as-prepared samples, and it indicated that lanthanide doping can improve the efficiency of interfacial adsorption of TiO_2 samples. The trend was the same as that of photocatalytic activity.

1. Introduction

Synthetic dyes are the major industrial pollutants and water contaminants [1]. Textile wastewater introduced intensive color and toxicity to the aquatic system. Reactive dyes are widely used in the textile industries. In China, more than $1.6 \times 10^9\ m^3$ per year of various dye wastewater is drained into rivers without satisfactory treatment, thus, depollution is the first concern [2,3]. Such colored dye effluents pose a major threat to the surrounding ecosystems, and apart from the environmental pollution, some of the dyes still pose documented health hazards. The toxicity and potentially carcinogenic nature of these substances represent an increasing danger in aquatic life. While due to the complex aromatic structure and stability of these dyes, conventional biological treatment methods are ineffective for degradation [4,5]. Some physical and chemical techniques are currently employed, but only limited success has been achieved [6,7]. The stringent international environmental standards (ISO 14001, October 1996) have prompted the need to develop novel treatment methods for converting organic contaminants [8].

Heterogeneous photocatalysis, as a promising advanced oxidation technology, has attracted much attention during the past several decades. It combines photochemistry and catalysis, and implies that light and catalyst are necessary to bring out a chemical reaction. Titanium dioxide (TiO_2) nanoparticles have been widely studied due to its remarkable photocatalytic activity for decomposing various organic pollutants [9]. However, prior to practical application, many problems need to be solved in TiO_2 photocatalytic system. Such as low photocatalytic efficiency and narrow spectrum responsive range ($\lambda < 388$ nm). Doping with other elements, such as rare metals and non-metals, has been widely used for TiO_2 modification to improve its photocatalytic activity or extend its light adsorption into visible region [10–12]. Since lanthanide ions are known for their ability to form complexes with various Lewis bases in the interaction of these functional groups with the f-orbitals of the lanthanides. Thus, incorporation of lanthanide ions in a TiO_2 matrix could provide a means to concentrate the organic pollutant at the semiconductor surface and therefore enhance the photoactivity of titania. Li et al. [13] and Zhou et al. [14] reported that both Ce-doping and Gd-doping titania exhibited enhanced photoactivity under UV or visible-light illumination. In the existent articles, preparation of metal-doped titania need high temperature treatment above 400 °C. However, the heat treatment can reduce the surface area and surface hydroxyl groups of TiO_2 nanoparticles. Furthermore, metal doping usually leads to thermal instability.

In this paper, cerium-doped TiO_2 and gadolinium-doped TiO_2 were prepared by sol–gel method under mild condition. The photocatalytic properties of as-prepared samples were investigated

* Corresponding author at: State Key Laboratory of Bioelectronics, Southeast University, Nanjing 210096, China. Tel.: +86 25 83794310; fax: +86 25 83793091.
E-mail addresses: xujj@seu.edu.cn (J. Xu), fudegang@seu.edu.cnb (D. Fu).

0304-3894/$ – see front matter © 2008 Elsevier B.V. All rights reserved.
doi:10.1016/j.jhazmat.2008.08.108

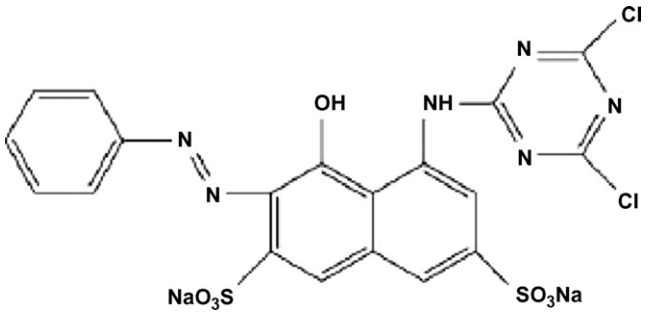

Fig. 1. The structure of the reactive brilliant X-3B.

under artificial solar and UV irradiation. An azo dye X-3B, who owns an azo bond (–N=N–), is used as a probe molecule. This dye has high solubility in water (80 g L^{-1}) and is red in color. The molecule structure was shown in Fig. 1. The degradation kinetics of X-3B was also investigated. The adsorption characterization of as-prepared samples was evaluated by Scatchard plot analysis.

2. Experimental

2.1. Materials

Titanium (IV) *n*-butoxide ($Ti(OBu)_4$) was chemical pure grade, and gadolinium oxide was analytical grade, both obtained from J&K China Chemical Ltd. Isopropanol (*i*-PrOH) was purchased from Shanghai Chemical Ltd. companies with chemical pure grade. The substrate of X-3B dye was obtained from Shanghai Dyestuff Chemical Plant and used without further purification. All the other reagents were of analytical grade, used without further treatments, and all obtained from Shanghai Reagent Company. Water used in the experiments was distilled.

2.2. Photocatalysts preparation

$Ti(OBu)_4$ was chosen as a Ti precursor, $(NH_4)_2Ce_2(NO_3)_6$ and Gd_2O_3 were used as Ce and Gd precursors, respectively. The doping source was first dissolved in water, whose pH value was adjusted to 2.0 by acid. The mixture of $Ti(OBu)_4$ and *i*-PrOH was then added gradually into the above solution under vigorous stirring, until $Ti(OBu)_4$ was hydrolyzed completely. The molar ratio of Ce/Ti ranged from 0.1 to 0.3%, and that of Gd/Ti ranged from 0.3 to 0.7%. Keeping the solution refluxing at 348 K for 24 h, we could get the modified TiO_2 sols. The sols were finally evaporated and dried at 333 K, thus Ce-doped TiO_2 and Gd-doped TiO_2 nanoparticles were obtained, respectively. The obtained samples were defined as CT-1, CT-2 and CT-3 for Ce-doped TiO_2 with Ce/Ti ratio 0.1, 0.2, and 0.3%, respectively. While Gd-doped samples were defined as GT-1, GT-2, and GT-3 for Gd/Ti molar ratio 0.3, 0.5, and 0.7%, respectively. Pure TiO_2 powders were also prepared in this paper. The process was the same as lanthanide-modified samples without adding doping source.

2.3. Characterization

The phase structure of samples was identified by X-ray diffractometer (XD-3A, Shimadazu Corporation, Japan) using graphite monochromatic copper radiation (Cu Kα) at 40 kV, 40 mA over the 2θ range 10–90°. The composition of different samples was measured by an energy dispersive X-ray analyzer (EDX, EDAX, USA) attached to the SEM. The specific surface area and pore size distribution of the samples were obtained using the Brunauer–Emmett–Teller (BET) surface area measuring apparatus at the boiling point of liquid nitrogen using an ASAP2020 instrument. The BET surface area was determined by multipoint BET method using the adsorption data in the relative pressure (P/P_0) range of 0.05–0.3. Desorption isotherm was used to determine the pore size distribution using the Barret–Joyner–Halender (BJH) method with cylindrical pore size. The nitrogen adsorption volume at the relative pressure (P/P_0) of 0.975 was used to determine the pore volume and average pore diameter. A UV–vis spectrophotometer (Shimadzu UV-4100) was used to record the diffuse reflectance spectra of titania samples.

2.4. Photocatalytic experiments

The photocatalytic activity of pure and lanthanide-modified TiO_2 nanoparticles were evaluated by photocatalytic degradation of reactive brilliant red dye X-3B solution. The detailed process was as following: 70 mg of TiO_2 sample was added into 200 mL X-3B solution with the concentration of 50 mg L^{-1}. The suspension was stirred in dark for 30 min to obtain adsorption equilibrium of X-3B before illumination. A 250 W halogen lamp (Instrumental Corporation of Beijing Normal University) was used as artificial solar light source. A UV-lamp (HG-250-UV Mejiro Precision Inc., $\lambda = 365$ nm, $P = 250$ W) was used as UV light source with the intensity of 2.1 mW/cm^2. At a defined time interval, 5 mL suspension was removed for analysis by HPLC. The HPLC system was Agilent 1100 with tunable absorbance detector adjusted at 270 nm for the detection of X-3B and its degradation intermediates. A reverse-phase column (length, 250 mm; internal diameter, 4.6 mm) Aglient Eclipse XDB-C18 was used. The mobile phase was composed of methanol and deionized doubly distilled water. The v/v ratio CH_3OH/H_2O was 70/30 and the flow rate was 0.6 mL min^{-1}.

2.5. Adsorption ability

A series of X-3B solution were prepared, with the initial concentration of 20, 25, 30, 40, 60, 80, and 100 mg L^{-1}, respectively. 70 mg of TiO_2 sample was added into 200 mL X-3B solution. In order to obtain adsorption equilibrium of X-3B and catalyst, the suspension was stirred in dark for 30 min. The absorbance of each solution was evaluated by UV–vis spectrophotometer. The characteristics of the adsorption process were investigated using Scatchard analysis.

3. Results and discussion

3.1. Characterization

3.1.1. XRD patterns

The phase behaviors of CT-2 and GT-2 samples were observed by XRD (Fig. 2). As shown, both the TiO_2 samples have very broad diffraction peaks, whose nature are due to their small grain size. The presence of peaks ($2\theta = 25.4°, 37.8°, 47.5°, 54.6°, 62.9°, 69.6°$) is regarded as anatase phase of TiO_2 [15]. Peak at $2\theta = 30.8°$ is usually considered as brookite phase. The doping Gd atoms do not cause any shift in peak position of TiO_2. It may due to Gd atoms just adsorb on the surface of TiO_2, or due to the very small doping amount lower than the detection limit. As for Ce-doped TiO_2, apart from the characteristic diffraction peaks of titania, relevant peaks ($2\theta = 30.8°$, 33.5°, 42.0°) are also observed in Fig. 2. It means that a new crystal phase is formed, corresponding to cerium titanate ($Ce_xTi_{1-x}O_2$) phase [16]. Partial replacement of Ti^{4+} ions by Ce^{4+} ions in TiO_2 lattice does not create any corresponding number of anion or cation vacancies, but results in the appearance of new crystal phase.

The size of the crystallites can be determined from the broadening of corresponding X-ray diffraction peaks by Scherrer's equation

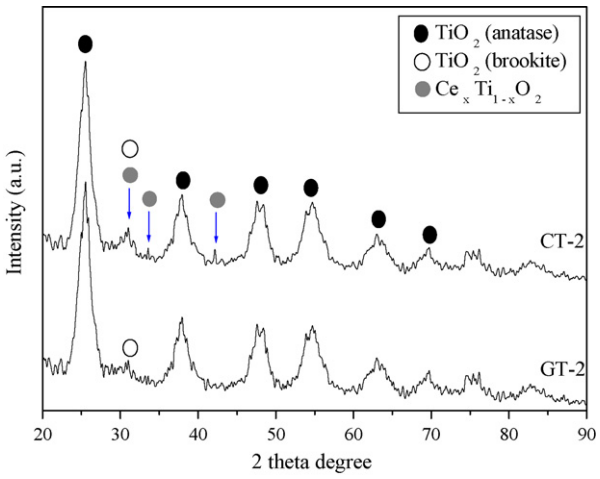

Fig. 2. XRD patterns of CT-2 and GT-2.

$D = 0.89\lambda/\beta\cos\theta$, where D is the crystal size, λ is the wavelength of X-ray radiation, β is the full width at half-maximum, and θ is the diffraction angle. The estimated grain sizes of anatase TiO_2 are 4.72 and 4.77 nm for CT-2 and GT-2, respectively.

The elemental compositions of the different samples were determined by EDX. The detailed process was according to Zhang and Lei [17]. Numerous dots (5 nm area) were selected for determining the doping element content of each sample, and then average value was calculated. The obtained values were listed in Table 1. From the table we can see that the content (at.%) of doping element (Ce or Gd) were all almost the same as the initial percent.

3.1.2. BET analysis

Fig. 3 shows the nitrogen adsorption–desorption isotherms of CT-2, and GT-2. As seen, the isotherm of both lanthanide-modified samples shows a combination of type I and IV (BDDT classification) [18] with two very distinct regions. At low relative pressure, the isotherm exhibits high adsorption, indicating that as-prepared samples contain micropores (type I). While at high relative pressure from 0.4 to 1.0, the curve exhibits a very small hysteresis loop, indicating the presence of mesopores (type IV). Fig. 4 shows the pore diameter distribution curve of both samples. It can be seen that the diameter of pore ranged from 1.8 to 4.0 nm, and the average pore diameter was 2.5 and 2.4 nm for CT-2 and GT-2, respectively. The formation of mesoporous structure in the samples is attributed to the aggregation of TiO_2 particles [19,20]. As seen from Table 2, GT-2 shows larger BET surface area and pore volume than that of CT-2. The result can be attributed to the reason that the bigger crystallites aggregation can form bigger pores [20]. It can also be confirmed by the value of pore volume, as the bigger pore size, the smaller pore volume.

3.1.3. Diffuse reflection spectra

The UV–vis absorption spectra of the modified titania and pure titania are shown in Fig. 5. The absorption threshold of pure titania is 385 nm. It presents a strong absorption band only in UV region, which attributes to the band–band transition. While for lanthanide-modified samples, both CT-2 and GT-2 exhibit extended absorption range to visible region, and yielding a large red shift for these lanthanide-modified samples compared to pure TiO_2. It may due to the increase in crystallinity [21]. Or it may attribute to the appearance of a new electronic state in the middle of the TiO_2 band-gap, the distance of charge transfer between f electrons of the rare earth ions and the conduction or valence band of TiO_2 was narrowed, accordingly, leading to visible-light absorption response [22,23]. Thus, the photocatalytic activity would be enhanced under visible illumination. While in the UV region, a little increase in the absorbed intensity of modified titania samples are found. Since lanthanide can used as electron trapper, which would decrease the recombination rate of photo-generated electron–hole pairs. Accordingly, it can be hypothesized that photocatalytic activity of these Gd-doped samples may be enhanced under UV illumination.

Table 1
Content (at.%) analysis by EDX for doping elements

Samples	Content (at.%)
CT-1	0.11
CT-2	0.22
CT-3	0.32
GT-1	0.31
GT-2	0.53
GT-3	0.73

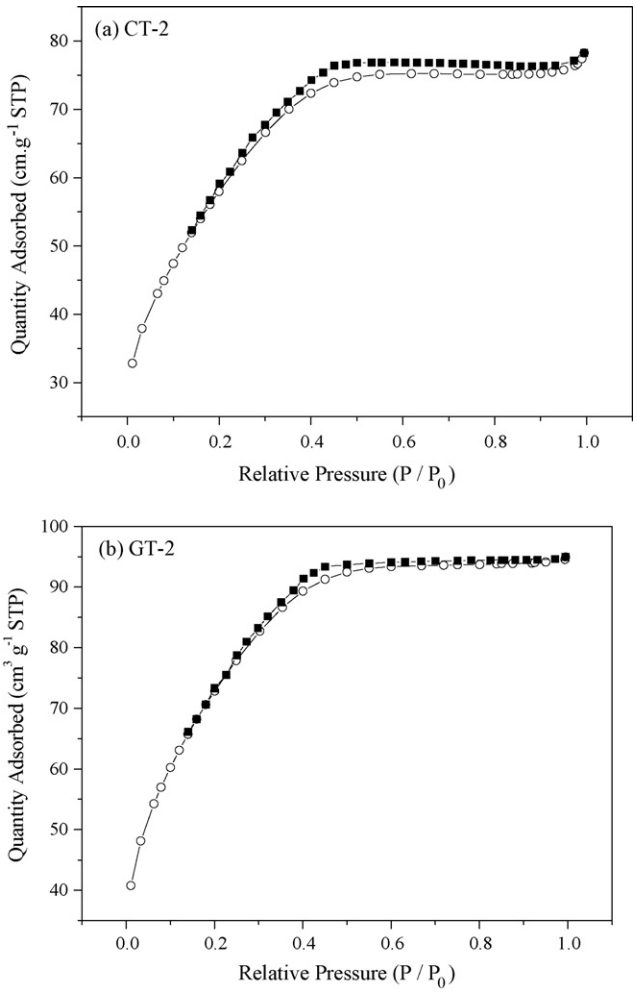

Fig. 3. Adsorption–desorption isotherm of (a) CT-2 and (b) GT-2.

3.2. Photocatalytic activity

As shown in Fig. 6(a), the photocatalytic degradation of X-3B by Ce-doped TiO_2 with different doping amounts was studied. The blank experiments without catalysts of degradation X-3B solution under the same condition are compared in this study. The blank study indicated that the merely photolysis can be ignored as it is about 0.9 and 1.2%, after illuminated for 80 min under solar and

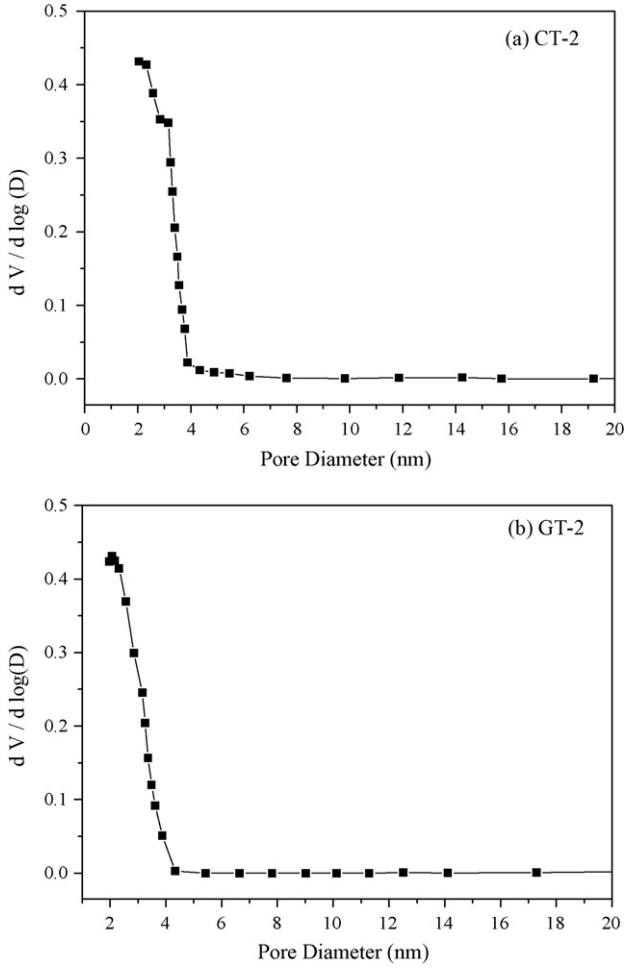

Fig. 4. Pore diameter distribution of (a) CT-2 and (b) GT-2.

UV illumination, respectively. After 80 min photo-degradation reaction under UV light irradiation, 43.5, 57.6, 47.5 and 55.8% of X-3B were decomposed for CT-1, CT-2, CT-3 and pure titania, respectively. While under artificial solar light illumination, the corresponding decomposed X-3B was 35.0, 45.9, 41.2 and 27.1%, respectively. It is well known that photocatalytic oxidation of organic pollutants in aqueous suspension follows Langmuir–Hinshelwood model.

$$-\frac{dC}{dt} = \frac{k_r K_a C}{1 + K_a C} \quad (1)$$

where $(-dC/dt)$ is the degradation rate of X-3B, C is the X-3B concentration in the solution, t is reaction time, k_r is a reaction rate constant, and K_a is the adsorption coefficient of the reactant. K_aC is negligible when the value of C is very small. As a result, Eq. (1) can describe a first-order kinetics. Setting Eq. (1) at the initial conditions of the photocatalytic procedure, when $t = 0$, $C = C_0$, it can be described as follows:

$$\ln\left(\frac{C_0}{C}\right) = k_{app} t \quad (2)$$

Table 2
BET data for CT-2 and GT-2

	BET surface area (m^2/g)	Pore volume (cm^3/g)	Average pore size (nm)
CT-2	215.8	0.15	2.5
GT-2	236.4	0.17	2.4

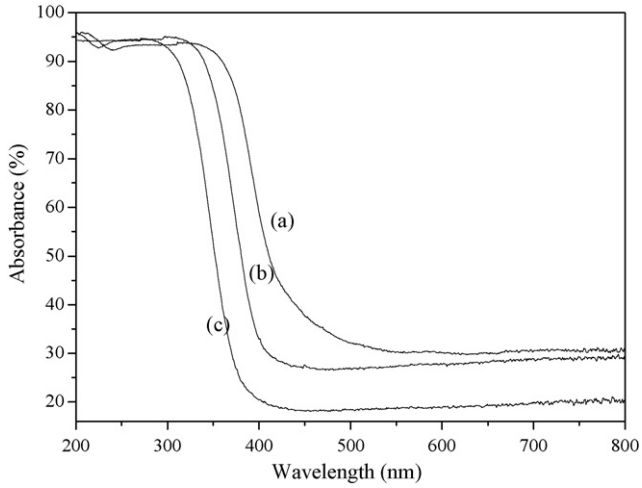

Fig. 5. Diffuse reflectance spectra of (a) CT-2, (b) GT-2, and (c) pure TiO_2.

where k_{app} is the apparent rate constant, used as the basic kinetic parameter for the different photocatalysts, since it enables one to determine a photocatalytic activity independent of the previous adsorption period in the dark and the concentration of X-3B remaining in the solution [24]. The variations in $\ln(C_0/C)$ as a function of irradiation time for Ce-doped samples are given in Fig. 6(b),

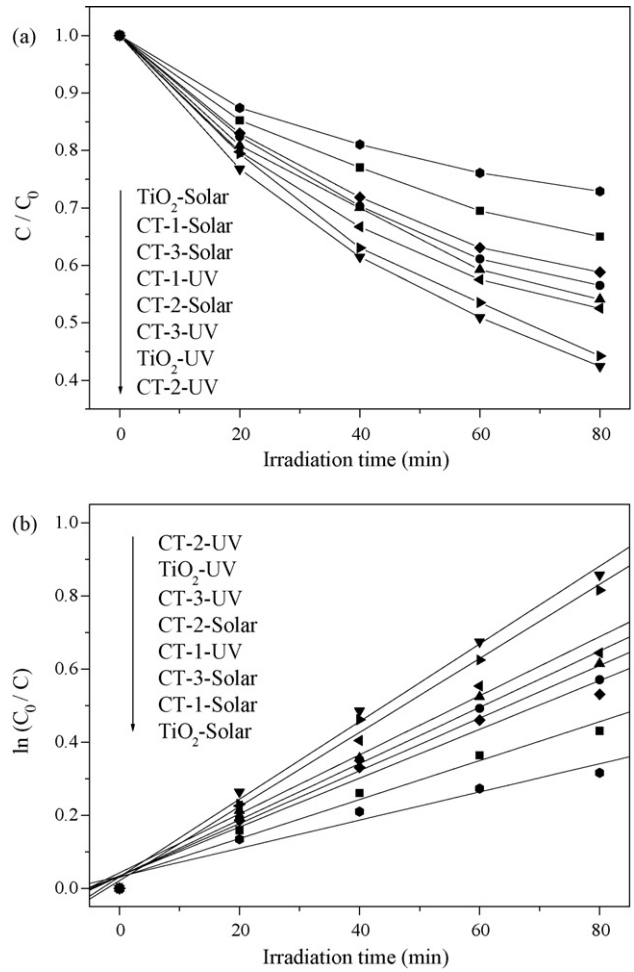

Fig. 6. (a) Kinetic of X-3B degradation for Ce-doped TiO_2 samples and (b) variations in $\ln(C_0/C)$ as a function of irradiation time and linear fits of Ce-doped TiO_2 samples.

Table 3
Apparent rate constant k_{app} and correlative coefficient R data for each sample under (a) solar and (b) UV illumination

	CT-1	CT-2	CT-3	GT-1	GT-2	GT-3	Pure TiO_2
(a) Solar							
Apparent rate constant, k_{app} (min^{-1})	0.0053	0.0077	0.0067	0.0070	0.010	0.0057	0.0039
Regression relative coefficient, R	0.989	0.992	0.988	0.993	0.998	0.988	0.980
(b) UV							
Apparent rate constant, k_{app} (min^{-1})	0.0072	0.011	0.0081	0.012	0.014	0.0078	0.010
Regression relative coefficient, R	0.989	0.996	0.988	0.997	0.997	0.993	0.997

and their corresponding k_{app} and R (regression relative coefficient) are given in Table 3. For Gd-doped samples, the results of photocatalytic degradation of X-3B are shown in Fig. 7(a). It can be seen that the degradation percentage of X-3B was 60.0, 69.1, and 46.1%, under UV illumination, and 43.9, 55.8, and 36.5% under solar light irradiation for sample GT-1, GT-2 and GT-3, respectively. The variations in $\ln(C_0/C)$ as a function of irradiation time for Gd-doped samples are given in Fig. 7(b), and their corresponding k_{app} and R are also given in Table 3.

From the results we can see that, CT-2 exhibited the highest photocatalytic activity either under UV or under solar irradiation among the Ce-doped samples. While for Gd-doped samples, GT-2 shows the highest activity. Furthermore, all samples exhibited higher activity under UV than under artificial solar light illumination. It could be explained that, as we know, photoreaction is initiated by the electron and hole via the excitation of photons. The generation and separation of electron/hole pairs, and the transformation of photons to carriers, i.e., quantum efficiency, both are crucial factors in the reaction [25]. The solar light source used in this study is low intensity light. The solar light intensity is much lower than that of UV light in the present work. Since the electron generation capacity mainly depends upon the intensity of incident photons with matchable energy. Further, as lanthanide ions acted as electron trap, for samples with lower doping amounts, the decomposition rate increases with the increasing cerium. The degradation rate showed a maximum when the dopant amount for Ce-doped sample and Gd-doped sample reached 0.2 and 0.5 at.%, respectively. With further increasing of lanthanide amount, they became the recombination center of electron–hole pairs, therefore, the decomposition ratio decreased, and the results were in agreement with other investigators [13,26].

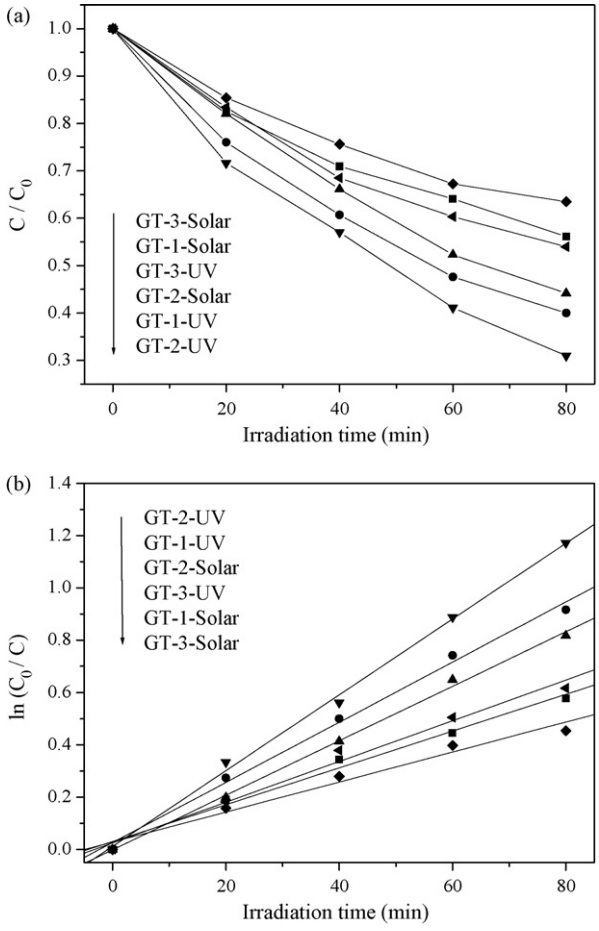

Fig. 7. (a) Kinetic of X-3B degradation for Gd-doped TiO_2 samples and (b) variations in $\ln(C_0/C)$ as a function of irradiation time and linear fits of Gd-doped TiO_2 samples.

From the results we can also see: under UV illumination, the activity of lanthanide-modified TiO_2 sample with appropriate amount of doping element was a little higher than that of pure TiO_2. It can be explained that as for lanthanide-doped sample, the 4f level plays an important role in interfacial charge transfer and elimination of electron–hole recombination. Lanthanide ions could act as an effective electron scavenger to trap the CB electrons of TiO_2. Furthermore, some of the Ti^{4+} was substituted by the doping element. This substitute creates a charge imbalance, which must be satiated. Therefore, more hydroxide ions would be adsorbed on the surface. The hydroxide ions act as hole traps that inhibit electron/hole pairs recombination as well. Interfacial charge transfer should be a determining-rate step for photocatalytic reaction [27]. And thus the as-prepared samples exhibit higher photocatalytic activity.

While under artificial solar light irradiation, both lanthanide-doped samples exhibit much higher activity than that of pure one, indicating that lanthanide modifying is helpful to improve photocatalytic activity. Since the lanthanide ions may partially substitute Ti^{4+} to form Ti–O–Ln (Ln=Ce, Gd) structure, as many researches have reported [28–30]. It leads to the appearance of a new electronic state in the middle of the TiO_2 band-gap [10]. This introduces structural defects in TiO_2 lattice, and changes the band-gap energy. Thus, the excitation energy is expanded from UV to visible light. Electrons excited from VB by absorbing visible-light photons, could be captured by the inter-band trap site. In total, more electrons were captured than in pure TiO_2 under solar light. As a result, the presence of lanthanide ions doping in TiO_2 accelerates the interfacial electron transfer process, and exhibit better photocatalytic activity.

3.3. Adsorption characteristic of Ce-doped, Gd-doped, and pure TiO_2

Since heterogenerous photocatalytic reactions mainly occur at the interface of substrate and catalyst, thus, the interfacial adsorption effect and affinity property play important roles in reaction rate [31,32]. The effect of adsorption–desorption equilibrium was investigated between X-3B and different TiO_2 samples in aqueous solution under darkness. Scatchard equation (Eq. (3)) [33] is used

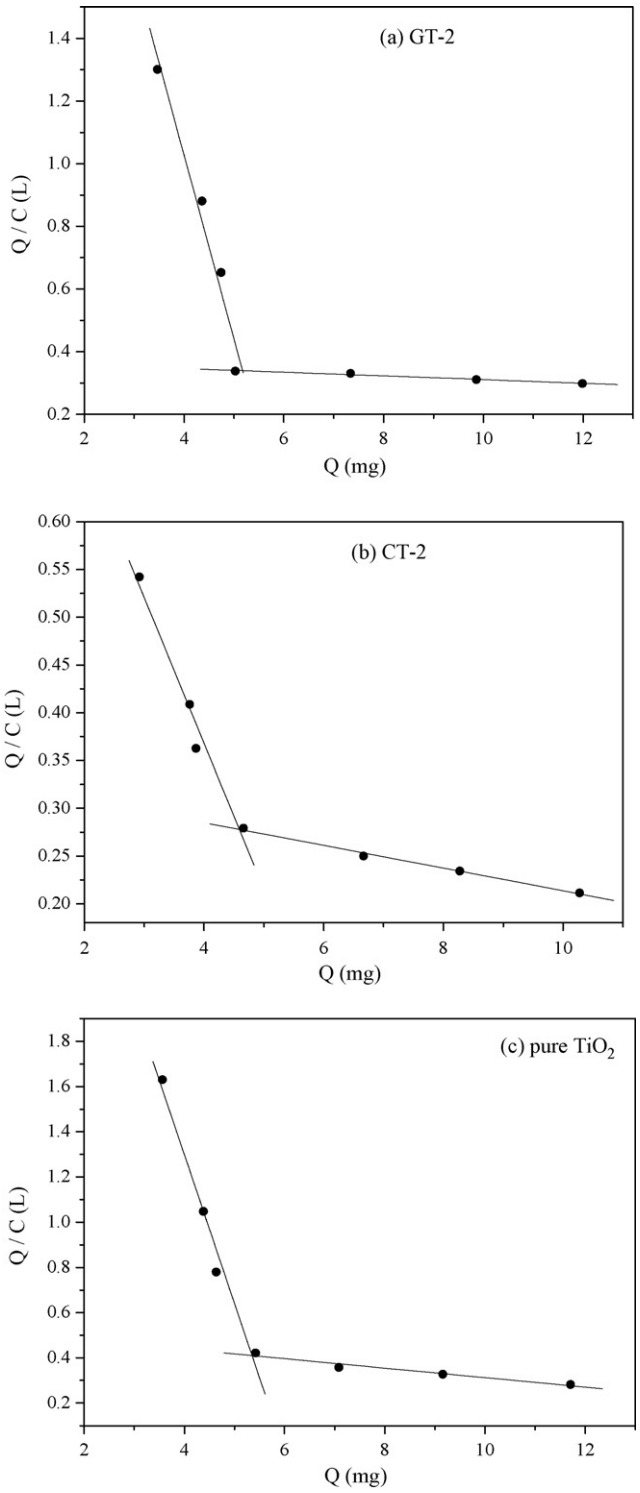

Fig. 8. Isothermal adsorption curve of (a) GT-2, (b) CT-2, and (c) pure TiO_2 samples.

to analyze the adsorption isotherms widely [34–36]:

$$\frac{Q}{C_e} = \frac{Q_{max} - Q}{K_d} \quad (3)$$

where C_e is the equilibrium concentration of substrate (X-3B) in the solution in mol L^{-1}, Q_{max} is the saturated adsorption amount in mg, and the K_d is the equilibrium adsorption constant. Fig. 8 shows the adsorption characteristics of lanthanide-doped sample (GT-2, CT-2) and pure TiO_2 in X-3B solution using Scatchard analysis. The

Table 4
Scatchard plot data of K_d, Q_{max}, and correlative coefficient R for each sample

	$K_{d,1}$ (mol L^{-1})	$Q_{max,1}$ (mg)	R_1	$K_{d,2}$ (mol L^{-1})	$Q_{max,2}$ (mg)	R_2
CT-2	6.5531	6.4115	0.987	84.0336	35.2560	0.997
GT-2	1.7042	5.7503	0.983	170.9402	63.2137	0.977
Pure TiO_2	1.5202	5.9737	0.990	47.6645	24.9047	0.978

Scatchard plots consist of two distinct linear sections with different slopes, which indicate that there exist two kinds of adsorption sites populated in the TiO_2 samples. The adsorption data could be fitted by two sites Langmuir isotherm model as follows [37]:

$$Q = \frac{Q_{max,1} C_e}{K_{d,1} + C_e} + \frac{Q_{max,2} C_e}{K_{d,2} + C_e} \quad (4)$$

The fitting data, such as K_d, Q_{max}, and correlative coefficient R are listed in Table 4. These results are in good agreement with BET analysis, which shows that there exist two pore structures, such as micropore and mesopore. The trend of saturation adsorption capacity was Gd-doped TiO_2 > Ce-doped TiO_2 > pure TiO_2, which was the same as that of photocatalytic activity. It indicates that lanthanide-modified samples exhibited higher adsorption capacity than pure TiO_2. It may due to the smaller size, larger specific surface area than the pure one. Furthermore, lanthanide ion could act as a Lewis acid as partial unoccupied 4f atomic orbits, and X-3B could act as a Lewis base because of π electrons conjugation structure of the azo-dye molecule. The formation of a Lewis acid–base complex between lanthanide ions and the dye also enhanced the interfacial adsorption effect. From photocatalytic experiments, it can be concluded that higher adsorption capacity lead to higher photocatalytic activity. Since more X-3B molecules could contact with TiO_2 sample with lanthanide doping.

4. Conclusions

Firstly, we prepared lanthanide-doped titania under mild condition (low temperature). The photocatalytic activity of Ce-doped TiO_2 and Gd-doped TiO_2 was higher than pure TiO_2 under either UV or artificial solar irradiation. The trend was as follows: 0.5 at.% Gd-doped TiO_2 > 0.2 at.% Ce-doped TiO_2 > pure TiO_2.

The photocatalytic degradation kinetics of X-3B in the presence of as-prepared samples was all in accordance with pseudo-first-order kinetics model well. The trend of apparent rate constant was as follows: 0.5 at.% Gd-doped TiO_2 > 0.2 at.% Ce-doped TiO_2 > pure TiO_2. The enhanced photocatalytic activity under visible illumination may due to the appearance of a new electronic state in the middle of the TiO_2 band-gap. While under UV irradiation, the reason may that lanthanide can used as electron trapper, which would decrease the recombination rate of photo-generated electron–hole pairs.

Scatchard analysis showed lanthanide-doped sample exhibited higher adsorption ability, due to the large specific surface area than pure one. The higher adsorption capacity leads to higher photocatalytic activity. Another reason is that lanthanide ion could act as a Lewis acid and X-3B could act as a Lewis base. The formation of a Lewis acid–base complex could also enhanced the interfacial adsorption effect.

Acknowledgement

This work is financially supported by the National Natural Science Foundation of China (No. 60121101) and Joint project of Guangdong Province and Education Department (No. 2007A090302018).

References

[1] M. Muruganandham, N. Shobana, M. Swaminathan, Optimization of solar photocatalytic degradation condition of reactive yellow 14 azo dye in aqueous TiO_2, J. Mol. Catal. A 246 (2006) 154–161.

[2] Y. Xu, Comparative studies of the $Fe^{3+/2+}$–UV, H_2O_2–UV, TiO_2–UV/vis systems for the decolorization of a textile dye X-3B in water, Chemosphere 43 (2001) 1103–1107.

[3] Y. Zhang, X. Dou, J. Liu, M. Yang, L. Zhang, Y. Kamagata, Decolorization of reactive brilliant red X-3B by heterogeneous photo-Fenton reaction using an Fe–Ce bimetal catalyst, Catal. Today 126 (2007) 387–393.

[4] N.H. Ince, D.T. Gonenc, Treatability of a textile azo dye by UV/H_2O_2, Environ. Technol. 18 (1997) 179–185.

[5] S. Sadhasivam, S. Savitha, K. Swaminathan, Feasibility of using *Trichoderma harzianum* biomass for the removal of erioglaucine from aqueous solution, World J. Microbiol. Biotechnol. 23 (2007) 1075–1081.

[6] P. Cooper, Removing colour from dyehouse wastewaters—a critical review of technology available, J. Soc. Dyers Colour. 109 (1993) 97–100.

[7] R.J. Davis, J.L. Gainer, G. O'Neal, I.-W. Wu, Photocatalytic decolorization of wastewater dyes, Water Environ. Res. 66 (1994) 50–53.

[8] M. Stylidi, D.I. Kondarides, X.E. Verykios, Pathways of solar light-induced photocatalytic degradation of azo dyes in aqueous TiO_2 suspensions, Appl. Catal. B 40 (2003) 271–286.

[9] A. Fujishima, T. Rao, A.D. Tryk, Titanium dioxide photocatalysis, J. Photochem. Photobiol. C 1 (2000) 1–21.

[10] Y. Xie, C. Yuan, Visible-light responsive cerium ion modified titania sol and nanocrystallites for X-3B dye photodegradation, Appl. Catal. B 46 (2003) 251–259.

[11] R. Asahi, T. Morikawa, T. Okwaki, K. Aoki, Y. Taga, Visible-light photocatalysis in nitrogen-doped titanium oxides, Science 293 (2001) 269–271.

[12] S.U.M. Khan, M. Al-Shahry, W.B. Ingler Jr., Efficient photochemical water splitting by a chemically modified *n*-TiO_2, Science 297 (2002) 2243–2245.

[13] F.B. Li, X.Z. Li, M.F. Hou, K.W. Cheah, W.C.H. Choy, Enhanced photocatalytic activity of Ce^{3+}–TiO_2 for 2-mercaptobenzothiazole degradation in aqueous suspension for odour control, Appl. Catal. A 285 (2005) 181–189.

[14] W. Zhou, Y. Zheng, G. Wu, Novel luminescent RE/TiO_2 (RE = Eu, Gd) catalysts prepared by in-situation sol–gel approach construction of multi-functional precursors and their photo or photocatalytic oxidation properties, Appl. Surf. Sci. 253 (2006) 1387–1392.

[15] L. Znaidi, R. Seraphimova, A semi-continuous process for the synthesis of nanosize TiO_2 powders and their use as photocatalysts, Mater. Res. Bull. 36 (2001) 811–825.

[16] M. Hirano, M. Inagaki, Preparation of monodispersed cerium (IV) oxide particles by thermal hydrolysis: influence of the presence of urea and Gd doping on their morphology and growth, J. Mater. Chem. 10 (2000) 473–477.

[17] X.W. Zhang, L.C. Lei, Effect of preparation methods on the structure and catalytic performance of TiO_2/AC photocatalysts, J. Hazard. Mater. 153 (2008) 827–833.

[18] K.S.W. Sing, D.H. Everett, R.A.W. Haul, L. Moscou, R.A. Pierotti, J. Rouquerol, T. Siemieniewska, Reporting physisorption data for gas/solid systems with special reference to the determination of surface area and porosity, Pure Appl. Chem. 57 (1985) 603–619.

[19] J.G. Yu, J.C. Yu, M.K.P. Leung, W.K. Ho, B. Cheng, X.J. Zhao, J.C. Zhao, Effects of acidic and basic hydrolysis catalysts on the photocatalytic activity and microstructures of bimodal mesoporous titania, J. Catal. 217 (2003) 69–78.

[20] L.Q. Jing, B.F. Xin, F.L. Yuan, L.P. Xue, B.Q. Wang, H.G. Fu, Effects of surface oxygen vacancies on photophysical and photochemical processes of Zn-doped TiO_2 nanoparticles and their relationships, J. Phys. Chem. B 110 (2006) 17860–17865.

[21] A.W. Xu, Y. Gao, H.Q. Liu, The preparation, characterization, and their photocatalytic activities of rare earth doped TiO_2 nanoparticles, J. Catal. 207 (2002) 151–157.

[22] C. Belver, R. Bellod, S.J. Stewart, F.G. Requejo, M. Fernández-García, Nitrogen-containing TiO_2 photocatalysts. Part 1. Synthesis and solid characterization, Appl. Catal. B 65 (2006) 309–314.

[23] J.G. Yu, M.H. Zhou, B. Cheng, H.G. Yu, X.J. Zhao, Ultrasonic preparation of mesoporous titanium dioxide nanocrystalline photocatalysts and evaluation of photocatalytic activity, J. Mol. Catal. A 227 (2005) 75–80.

[24] J. Matos, J. Laine, J.M. Herrmann, Synergy effect in the photocatalytic degradation of phenol on a suspended mixture of titania and activated carbon, Appl. Catal. B 18 (1998) 281–291.

[25] X.G. Hou, F.H. Hao, B. Fan, X.N. Gu, X.Y. Wu, A.D. Liu, Modification of TiO_2 photocatalytic films by V^+ ion implantation, Nucl. Instrum. Method Phys. Res. B 243 (2006) 99–102.

[26] D. Zhao, T.Y. Peng, M. Liu, L.L. Lu, P. Cai, Fabrication, characterization and photocatalytic activity of Gd^{3+}-doped titania nanoparticles with mesostructure, Micropor. Mesopor. Mater. 114 (2008) 166–174.

[27] H. Liu, X.Z. Li, Y.J. Leng, W.Z. Li, An alternative approach to ascertain the rate-determining steps of TiO_2 photoelectrocatalytic reaction by electrochemical impedance spectroscopy, J. Phys. Chem. B 107 (2003) 8988–8996.

[28] R. Nakamura, A. Okamoto, H. Osawa, H. Irie, K. Hashimoto, Design of all-inorganic molecular-based photocatalysts sensitive to visible light: Ti(IV)–O–Ce(III) bimetallic assemblies on mesoporous silica, J. Am. Chem. Soc. 129 (2007) 9596–9597.

[29] M. Zalas, M. Laniecki, Photocatalytic hydrogen generation over lanthanides-doped titania, Sol. Energy Mater. Sol. Cells 89 (2005) 287–296.

[30] Y. Xie, C. Yuan, Photocatalysis of neodymium ion modified TiO_2 sol under visible light irradiation, Appl. Surf. Sci. 221 (2004) 17–24.

[31] F.Y. Oliva, L.B. Avalle, O.R. Cámara, C.P. De Pauli, Adsorption of human serum albumin (HSA) onto colloidal TiO_2 particles, Part I, J. Colloid Interf. Sci. 261 (2003) 299–311.

[32] Y. Xie, C. Yuan, X. Li, Photosensitized and photocatalyzed degradation of azo dye using Ln^{n+}–TiO_2 sol in aqueous solution under visible light irradiation, Mater. Sci. Eng. B 117 (2005) 325–333.

[33] H.I. Yamamura, S.J. Enna, M.J. Kuhar, Neurotransmitter Receptor Binding, Raven Press, New York, 1985, pp. 80–86.

[34] Y. Gonen, G. Rytwo, A full analytical solution for the sorption–desorption kinetic process related to langmuir equilibrium conditions, J. Phys. Chem. C 111 (2007) 1816–1819.

[35] O. Gezici, M. Küçükosmanoglu, A. Ayar, The adsorption behavior of crystal violet in functionalized sporopollenin-mediated column arrangements, J. Colloid Interf. Sci. 304 (2006) 307–316.

[36] A. Öztürk, Removal of nickel from aqueous solution by the bacterium *Bacillus thuringiensis*, J. Hazard. Mater. 147 (2007) 518–523.

[37] S.L. Yan, Y.J. Fang, W. Yao, Z.X. Gao, Characterization and quality assessment of binding properties of the monocrotophos molecularly imprinted microspheres prepared by precipitation polymerization in toluene, Polym. Eng. Sci. 23 (2007) 1302–1308.